Differences in pathways contributing to thyroid hormone effects on postnatal cartilage calcification versus secondary ossification center development

Authors: Gustavo A. Gomez[1], Patrick Aghajanian[2], Sheila Pourteymoor[1], Destiney Larkin[1], Subburaman Mohan[1345*]

Affiliations: [1] Musculoskeletal Disease Center, Jerry L. Pettis VA Medical Center, Loma Linda, CA 92357, USA; [2] Fulgent Genetics, El Monte, CA 91733, USA; [3]Departments of Medicine, Loma Linda University, Loma Linda, CA 92354, USA; [4] Departments of Biochemistry, Loma Linda University, Loma Linda, CA 92354, USA; [5] Departments of Physiology, Loma Linda University, Loma Linda, CA 92354, USA.

Funding: This work was supported by National Institutes of Health Grant R01 AR048139 (SM), R21 AG062866 (SM) and Veterans Administration BLR&D Grant BX005263 (SM). SM is a recipient of Senior Research Career Scientist Award from Veterans Administration.

Emails:

- Gustavo A. Gomez: Gustavo.Gomez2@va.gov, ORCID:0000-0001-9294-4276
- Patrick Aghajanian: jedirabiz@gmail.com
- Sheila Pourteymoor: Sheila.Pourteymoor@va.gov
- Destiney Larkin: Destiney.Larkin@va.gov
- Subburaman Mohan: Subburaman.Mohan@va.gov, ORCID:0000-0003-0063-986X

***Corresponding Author:**
Subburaman Mohan, Ph.D., Musculoskeletal Disease Center, Research Service, VA Loma Linda Healthcare Systems, 11201 Benton Street, Loma Linda CA 92357, USA; Tel. +1-909-825-7084 X6180; Email: Subburaman.Mohan@va.gov

Key Words: thyroid hormone, endochondral bone formation, cartilage calcification, chondrocytes, osteoblasts, femoral head

Supplementary Material: This manuscript contains supplementary information, figures and tables

Disclosure: The authors have declared that no conflict of interest exists.

Abstract

The proximal and distal femur epiphysis of mice are both weight bearing structures derived from chondrocytes but differ in development. Mineralization at the distal epiphysis occurs in an osteoblast rich secondary ossification center (SOC), while the chondrocytes of the proximal femur head (FH) in particular, are directly mineralized. Thyroid hormone (TH) plays important roles in distal knee SOC formation, but whether TH also affects proximal FH development remains unexplored. Here, we found that TH controls chondrocyte maturation and mineralization at the FH *in vivo* through studies in *Thyroid stimulating hormone receptor* (*Tshr* $^{-/-}$) hypothyroid mice by X-ray, histology, transcriptional profiling, and immunofluorescence staining. Both *in vivo,* and *in vitro* studies conducted in ATDC5 chondrocyte progenitors concur that TH regulates expression of genes that modulate mineralization (*Bsp*, *Ocn*, *Dmp1*, *Opn*, and *Alp).* Our work also delineates differences in prominent transcription factor regulation of genes involved in the different mechanisms leading to proximal FH cartilage calcification and endochondral ossification at the distal femur. The information on the molecular pathways contributing to postnatal cartilage calcification can provide insights on therapeutic strategies to treat pathological calcification that occurs in soft tissues such as aorta, kidney, and articular cartilage.

Introduction

Bones make up the infrastructure of the body and are formed through a process known as ossification. Most bones are formed by endochondral ossification where condensed mesenchymal stem cells (MSCs) proliferate and differentiate into chondrocytes. Ossification first occurs in the mid-shaft of the bone, which forms the primary center of ossification (POC) and expands towards the ends of the cartilage matrix. In mice, the POC has been established to occur during embryonic development day (E) E14.5 – 15.5 while the secondary ossification center (SOC) forms at approximately postnatal day (P) 5-7 at the epiphyseal ends (Mackie, Tatarczuch, & Mirams, 2011). Each stage of skeletal development from chondrocytes can be characterized by the expression level of specific genes. Early chondrocytes which are characterized by expression of collagen type 2 (COL2), and Aggrecan (ACAN) undergo proliferation, withdraw from the cell cycle, and differentiate into pre-hypertrophic chondrocytes expressing Indian hedgehog (IHH) and Osterix (OSX). Hypertrophic chondrocytes express high levels of a cartilage matrix consisting of matrix metalloproteinase 13 (MMP13) and collagen type 10 (COL10), creating a template for bone formation. Expression of vascular endothelial growth factor (VEGF) subsequently leads to invasion by capillaries, which allows the influx of osteoblasts, osteoclasts, and bone marrow cells to replace the cartilage matrix with mineralized bone (Li & Dong, 2016; Mackie et al., 2011; Takarada et al., 2016). The growth plate is responsible for longitudinal skeletal growth and skeletal maturity is reached when the primary and secondary ossification centers meet (Mackie et al., 2011).

Thyroid hormone (TH) is an important regulator of skeletal growth and development. Optimal levels of TH peak simultaneously with the initiation of SOC formation and are essential for its development (Aghajanian, Xing, Cheng, & Mohan, 2017; Kim & Mohan, 2013; Xing, Cheng, Wergedal, & Mohan, 2014). Dysregulation in the amount of TH during skeletal development can lead to growth arrest, and delayed bone formation in both humans and mice (Bassett et al., 2008; Gogakos, Duncan Bassett, & Williams, 2010; Kim & Mohan, 2013). Previous work from our group has substantiated the importance of TH in bone formation. We found that TH regulates the development of the SOC through IHH signaling and OSX activity, and that TH is a major regulator of a number of key bone growth factors, including insulin-like growth factor-I (IGF-1) (Mohan

et al., 2003; L. Wang, Shao, & Ballock, 2010; Y. Wang et al., 2006). We also established that TH deficient *Tshr*$^{-/-}$ mice have severely compromised development of the epiphysis in both the femur and tibia at the knee joint, which is completely rescuable by TH treatment for 10 days when serum levels of TH rise in wild type mice (Xing et al., 2014). Additionally, we found that TH regulates SOC formation at the epiphysis of the distal femur and proximal tibia, by a TH induced chondrocyte-to-osteoblast transdifferentiation mechanism (Aghajanian et al., 2017).

Previous studies have revealed that bone development culminates at a later timepoint in the proximal femur relative to the distal femur, suggesting a difference in developmental mechanisms (Patton & Kaufman, 1995). A recent study in mice by Cole et al. (2013) found that the proximal and distal femur had different developmental patterns in terms of timing, vascular development, and ossification. While the cartilage template at the distal epiphysis was replaced by bone matrix via a chondrocyte-to-osteoblast transdifferentiation-mediated endochondral ossification process, at the proximal femoral epiphysis cartilage was directly mineralized without the involvement of an SOC (Cole et al., 2013). In this work, we examined whether TH is also involved in regulating cartilage mineralization at the proximal femur epiphysis and the mechanisms for the differential effects of TH-mediated endochondral ossification at the epiphyseal structures of the knee versus direct cartilage mineralization at chondrocytes of the femur head. Our findings demonstrate for the first time, the mechanisms that contribute to differential development of the proximal versus distal femur, providing novel information on the physiological and conceivably, pathological means of soft tissue mineralization.

Results

TH is necessary for mineralization of the proximal femur head

In order to determine whether the cartilage mineralization that occurs at the proximal femur of mice (Cole et al., 2013) is dependent on TH signaling, we evaluated the hip joints of hypothyroid *Tshr*$^{-/-}$ and euthyroid *Tshr*$^{+/-}$ mice on day 21. X-ray imaging of genotyped mice revealed that compared with the tight apposition of the femur head (FH) with the acetabulum of the pelvic bone in *Tshr*$^{+/-}$ heterozygotes, a distinct gap was evident between the FH and acetabulum in *Tshr*$^{-/-}$ mice (Figure 1A). Given that injection of TH on days 5-14 restores the SOC defect at the distal femur (Xing et al., 2014), we tested whether the defect observed at the proximal femur is also directly dependent on TH. While all three of the proximal femur structures (greater trochanter, femur head and lesser trochanter) were underdeveloped in *Tshr*$^{-/-}$ injected with vehicle compared to *Tshr*$^{+/-}$ control mice (Figure 1B), restoration of all three structures in *Tshr*$^{-/-}$ injected with

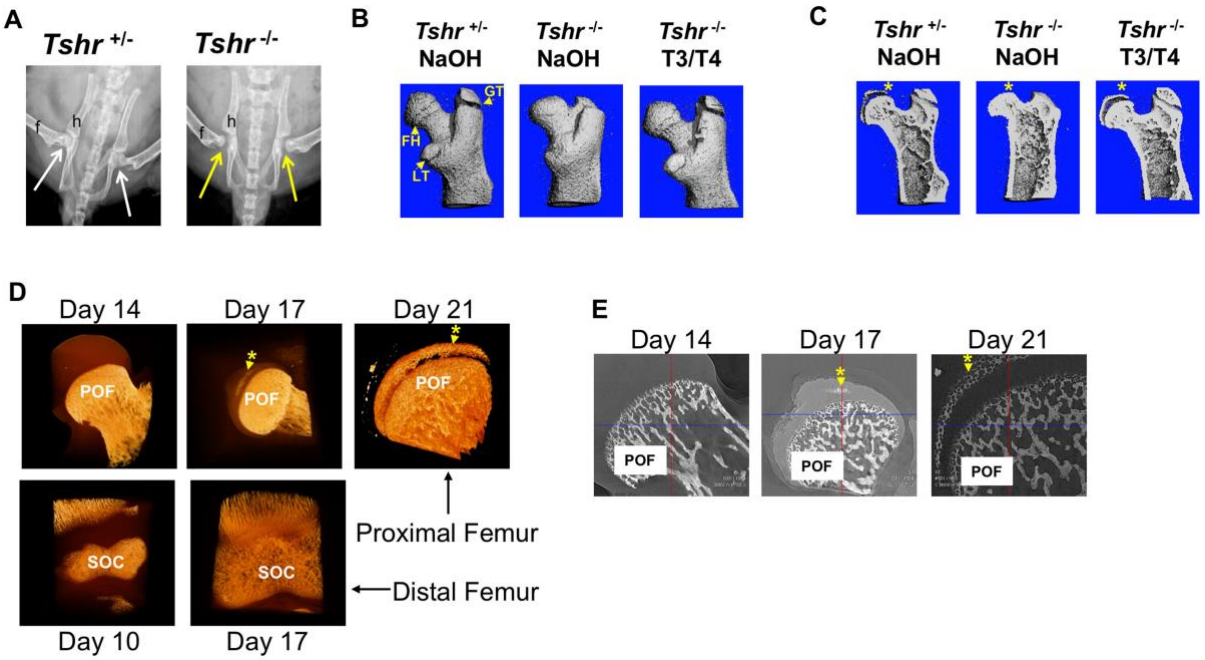

Figure 1. *Tshr*$^{-/-}$ proximal femur phenotype and onset of mineralization
(Panel A) Ventral X-ray view of postnatal (P)21 day old mice. Arrows point to joint between hip (h) and femur (f). (Panel B) Lateral view of 3 dimensional μCT scans from P21 proximal femurs. FH = Femur Head, GT = Greater Trochanter; LT = Lesser Trochanter. (Panel C) Lateral μCT hemi-section view of proximal femurs. Asterisk adjacent to region mineralized in FH. (Panel D) Lateral views of 3D nano-CT images of proximal FH (top row), and distal femur epiphysis (bottom row). Mineralized tissue is opaque ivory/gold colored. (Panel E) 2 dimensional sections of nano-CT. Mineralized tissue is white/bright grey. POF: Primary Ossification Front, SOC: Secondary Ossification Center. Asterisk and arrow point to mineralization at Femur head. Images shown are representative of 3-5 mice per group.

T3/T4 indicates TH signaling also regulates development and mineralization of the proximal femur epiphysis (Figure 1C).

Although mineralization of both distal femur and proximal tibia epiphysis initiates by the end of the first week after birth in mice (Aghajanian et al., 2017; Mackie et al., 2011), the time at which mineralization initiates in the proximal femur epiphysis remains poorly defined. Consequently, we evaluated the earliest appearance of mineralization in proximal FH cartilage in *Tshr* $^{+/-}$ control mice by high resolution nano-computed tomography (nano-CT). Our data revealed a 10 day delay in the initiation of mineralization at the FH compared to the distal femoral epiphysis (Figure 1D,E).

FH cartilage mineralization is delayed in hypothyroid mice

To further characterize the tissue mineralized at the FH, longitudinal sections of proximal femurs of euthyroid *Tshr*$^{+/-}$ and hypothyroid *Tshr*$^{-/-}$ mice were compared at P10 and P21 by histology staining for cartilage (Safranin O and toluidine blue), bone (Von Kossa) and mineral (Alizarin red). Relative to *Tshr*$^{+/-}$ controls, the cartilage area was greater at the proximal FH in *Tshr*$^{-/-}$ mice (Figure 2A,B). In the proximal FH, alizarin red and Von Kossa mineral staining were only detected on day 21 of *Tshr*$^{+/-}$ controls (Figure 2C, D), which corroborates nanoCT results. The proximal FH of *Tshr*$^{-/-}$ is eventually mineralized in more mature mice (Figure 2 Supplement1). Conversely, extensive mineral staining was seen at the distal femur SOC in euthyroid mice at both time points, but to a reduced extent in the distal femur SOC of *Tshr* $^{-/-}$ mice on day 21 (Figure 2C,D). Interestingly, positive staining for tartrate resistant acid phosphatase (TRAP) was found in the actively mineralizing region of distal femur SOC (Figure 2E), which was also dependent on TH status. However, TRAP staining was not detected in the FH of either genotype, even on day 21. These data suggest that while TH seems to play an important role in the mineralization of proximal FH as in the case of the distal femur, there are important differences in when mineralization occurs, and the type of tissue being mineralized at both ends.

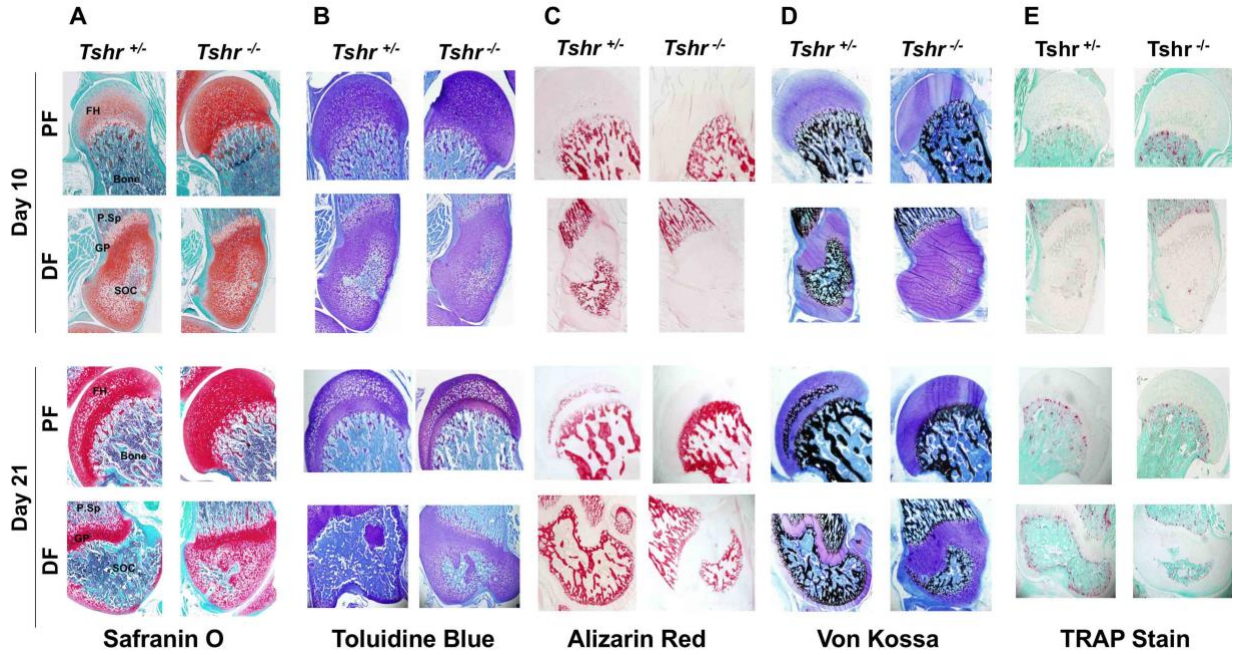

Figure 2. Histological analysis of FH in euthyroid *Tshr*$^{+/-}$ and hypothyroid *Tshr*$^{-/-}$ mice. Safranin O stained sections showing cartilage in red (Panel A), Toluidene blue stained sections showing cartilage in violet (Panel B), Alizarin red stained sections showing mineral in red (Panel C), Von Kossa stained sections showing mineral in black (Panel D), and TRAP stained sections showing TRAP activity in red (Panel E) at the proximal femur, PF, and distal femur, DF, from *Tshr*$^{+/-}$ and *Tshr*$^{-/-}$ mice. P.Sp = primary spongiosa; GP = growth plate; SOC = secondary ossification center.

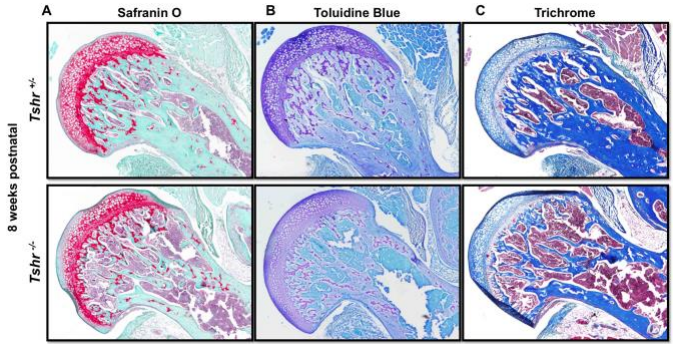

Figure 2 Supplement 1. Delayed mineralization in *Tshr*$^{-/-}$ FH. Postnatal week 8 proximal femur sections stained in red for Safranin O (Panel A), Violet for Toluidine Blue (Panel B), dark blue-mineral, light blue-collagen, red-nuclei for Trichrome (Panel C).

Transcription profiles reveal delay in chondrocyte maturation in FH of *Tshr*$^{-/-}$ mice

Given that TH elicits distinct responses at proximal FH and distal femur epiphysis, which both develop from chondrocytes, we compared transcriptional changes of genes involved in chondrocyte/osteoblast maturation and ECM remodeling at both sites on days 10 and 21 between *Tshr*$^{+/-}$ controls and *Tshr*$^{-/-}$ mice that were treated with or without TH

by Reverse Transcriptase quantitative Polymerase Chain Reaction (RT-qPCR). A delay in maturation at both ends in day 10 hypothyroid femurs was evident by reduced mRNA levels of genes expressed in mature chondrocytes *Ihh*, *Rankl*, *Sp7/Osx*, *Col10*, *Alp* and *Mmp13* (Figure 3A-D). Moreover, markers of immature chondrocytes *Shh* and *Sox9* were increased, but only significantly at the FH (Figure 3A,B), indicating a more substantial delay in maturation of FH chondrocytes on day 10. TH treatment increased *Col10* expression in the distal femur but not proximal FH at day 10, further supporting a delay in chondrocyte maturation at the FH.

Furthermore, while expression levels of genes involved in mineralization, *Bsp*, *Opn* and *Trap2,* were reduced, *Mgp* expression was elevated at the distal femur of day 10 *Tshr*$^{-/-}$ mice, but none of these were affected in the FH (Figure 3C,D). These data are consistent with the histology data demonstrating active mineralization at distal but not proximal FH at this timepoint. Since others, and we, have shown a key role for hypoxia signaling in chondrocyte maturation (Cheng, Aghajanian, Pourteymoor, Alarcon, & Mohan, 2016; Cheng, Pourteymoor, Alarcon, & Mohan, 2017; Schipani et al., 2001; Yellowley & Genetos, 2019), we measured expression of hypoxia signaling genes and found that in day 10 *Tshr*$^{-/-}$ femurs the expression levels of *Hif1*α was unchanged at both the FH and distal femur (Figure 3A,B), while *Hif2*α and *Vegf* were reduced at the FH and not restored by TH treatment (Figure 3A,B). *Tgf*α expression was negatively regulated by TH at the FH but not at the distal femur (Figure 3A), thus suggesting region-specific effects of TH on the femur.

On day 21, femurs of hypothyroid mice continued to display profiles suggesting a delay in maturation. Expression levels of immature chondrocyte markers, *Sox9* and *Acan*, were increased at both ends, yet reduced by TH treatment (Figure 3F,G). While *Col2* mRNA levels were unchanged, *Col10* mRNA levels were reduced in the FH of *Tshr*$^{-/-}$ mice (Figure 3G). Increased mRNA levels of *Ihh* in both proximal and distal femurs of *Tshr*$^{-/-}$ mice were also restored to control levels by TH treatment, thus suggesting a role for *Ihh* in chondrocyte maturation. *Alp* and *Trap* transcripts were reduced at the proximal FH but not distal femur of *Tshr* $^{-/-}$ mice at day 21 and rescued by TH (Figure 3H). TH treatment produced opposite effects on *Bsp* expression at the two femoral sites in *Tshr*$^{-/-}$ mice on day 21. By contrast, the reduced *Ocn* mRNA levels at the proximal FH and distal

femur of *Tshr*$^{-/-}$ mice at day 21 were rescued by TH treatment (Figure 3G). Interestingly, expression levels of growth factors *Bmp2* and *Opg* were elevated at both ends of the femur in *Tshr*$^{-/-}$ mice on day 21 and rescued by TH treatment (Figure 3E). Although expression of *Runx2* and *β-cat* were not affected at either FH or distal femur (Figure 3F), TH treatment increased their expression at the FH only. Thus, while TH is required for continuous maturation of chondrocytes and affects common pathways, it can also differentially regulate distinct genes at the proximal FH and distal femur epiphysis.

To further characterize temporal changes of chondrocyte maturation at FH and distal femur, we compared changes in expression levels of genes in the FH relative to stage matched distal femurs on days 10 and 21 in *Tshr*$^{+/-}$ euthyroid mice. The reduced expression of *Ihh*, *Rankl*, *Osx*, *Mmp13*, *Bsp* and *Alp* (Figure 3I) at day 10 were consistent with the delayed maturation of chondrocytes at the proximal FH. However, at day 21, many of these genes were expressed at higher levels in the FH, a finding consistent with active mineralization occurring at this time. Therefore, transcriptional profile data reveals that chondrocytes are at a relatively more immature state in the FH of day 10 compared to day 21, and there was a catch up in maturation as noted by increased expression of genes associated with chondrocyte maturation and mineralization in the FH on day 21.

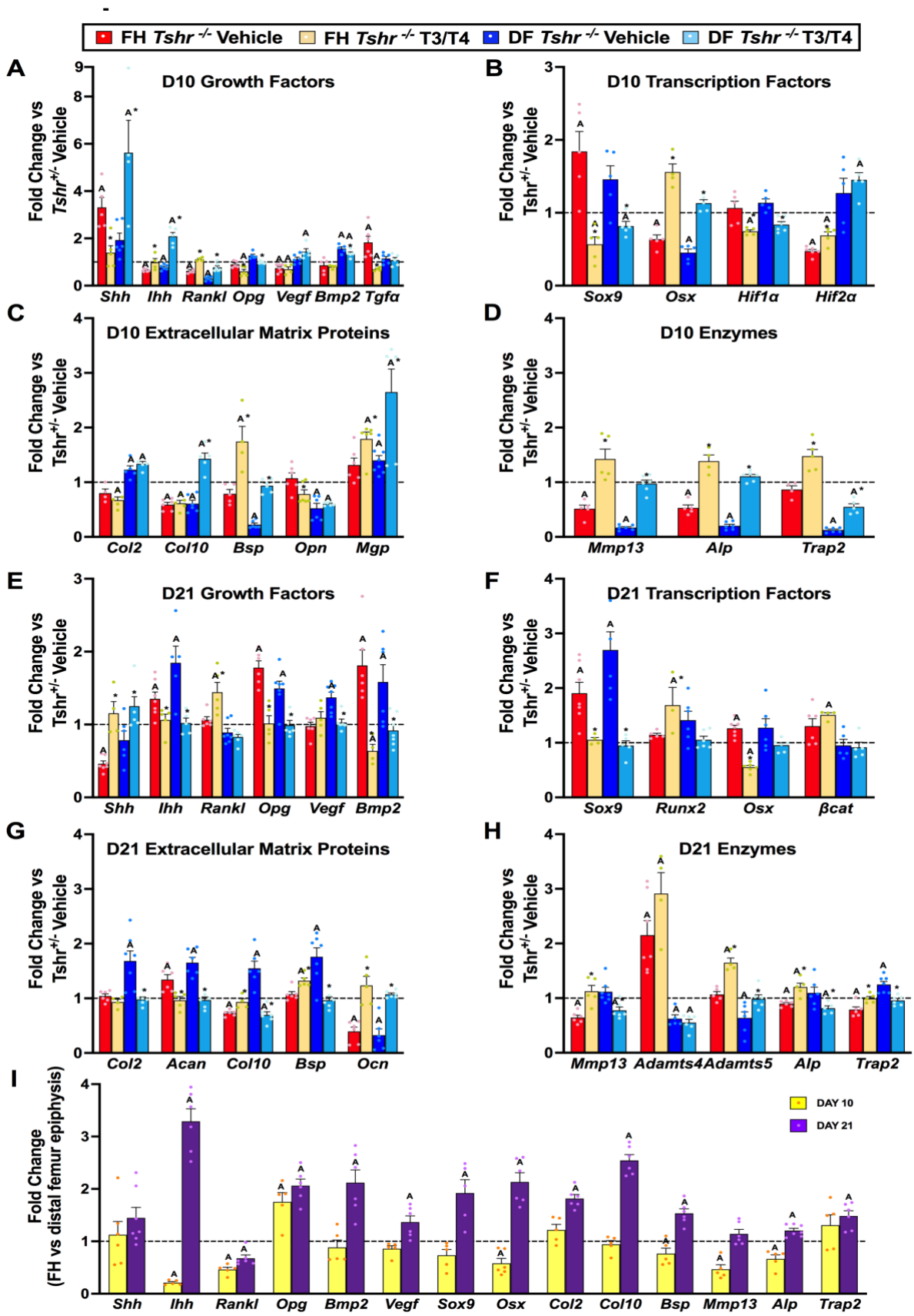

Figure 3. TH dependent transcriptional differences at proximal and distal femur.

(Panels A-G) Gene expression changes from Femur Head (FH) or Distal Femur (DF) between *Tshr*$^{-/-}$

injected with vehicle, or T3/T4, plotted as fold-change relative to anatomical and stage matched region in euthyroid *Tshr*$^{+/-}$ injected with vehicle (dashed line). Day 10 samples (Panels A-D) were treated on days 5-9, while day 21 samples (Panels E-G) were treated on days 5-14. (Panel I) Fold change of mRNA expression at FH vs DF epiphysis in *Tshr* $^{+/-}$ on days 10 and 21. Statistics analyzed by T-test where A = P<0.05, * = P<0.05 between T3/T4 treatment and Vehicle at FH or DF. (n=6) Sonic Hedgehog (*Shh*), Indian Hedgehog (*Ihh*), Rank ligand (*Rankl*), Osteoprotegerin (Opg), Vascular endothelial growth factor (*Vegf*), Bone morphogenetic protein 2 (*Bmp2*), Transforming growth factor α (*Tgf*α), SRY-Box Transcription Factor 9 (*Sox9*), Runt-Related Transcription Factor 2 (*Runx2*), Sp7 Transcription Factor (*Sp7/Osx*), Hypoxia Inducible Factor 1α (*Hif1*α), Hypoxia Inducible Factor 2α (*Hif2*α), Collagen Type II Alpha 1 (*Col2*), Collagen Type X Alpha 1 (*Col10*), Bone Sialoprotein II (*Bsp*), Osteopontin (*Opn*), Matrix Gla Protein (*Mgp*), Matrix Metallopeptidase 13 (*Mmp13*), Alkaline Phosphatase (*Alp*), Tartrate Resistant Acid Phosphatase (*Trap2*), Beta-Catenin (β*cat*), Aggrecan (*Acan*), ADAM Metallopeptidase with Thrombospondin Type 1 Motif 4 (*Adamts4*),ADAM Metallopeptidase with Thrombospondin Type 1 Motif 5 (*Adamts5*)

Spatio-temporal profile of protein expression in FH chondrocyte development

To further characterize the molecular mechanisms that contribute to the development of the FH, we performed a time-course spatiotemporal analysis of proteins that report different stages of chondrocyte and osteoblast maturation by immunohistology on *Tshr*$^{+/-}$ on days 10, 17, and 21, and in *Tshr*$^{-/-}$ on day 17, when FH mineralization commences. Antibody fidelity was determined by spatial domains of expression in the proximal tibia of day 10 *Tshr*$^{+/-}$, where active bone mineralization is underway, and occurs identically as in the distal femur.

We previously showed that expression of collagen proteins follows a linear progression of appearance whereby COL2 secretion by immature chondrocytes is followed by COL10 in pre-hypertrophic and hypertrophic chondrocytes, and COL1 in mineralizing osteoblasts during the second week of postnatal life at the distal femur and proximal tibia (Aghajanian et al., 2017; Xing et al., 2014). In the proximal FH, however, there was a delay in the expression of markers of chondrocyte differentiation as noted by the presence of COL2 in chondrocytes of day 10 FH, and subsequent replacement of COL2 with COL10 that persisted during active mineralization on day 17 (Figure 4A).

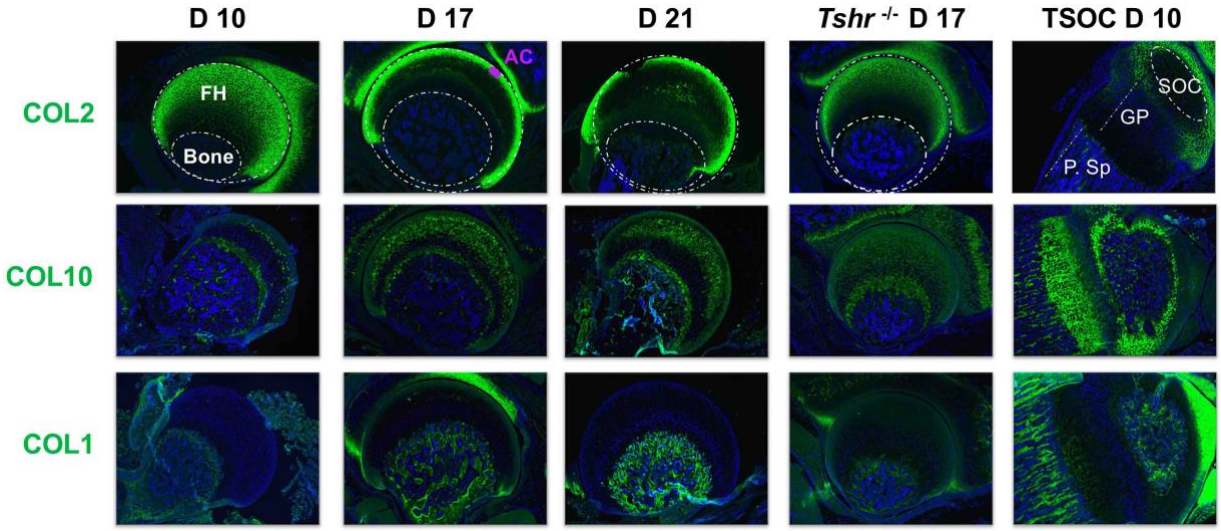

Figure 4A. Immunohistochemical characterization of FH development. Longitudinal sections of *Tshr*$^{+/-}$ mice were probed for protein expression in FH on Day 10, 17, 21, proximal tibia epiphysis on day 10, and FH of *Tshr*$^{-/-}$ on day 17 by immunofluorescence for collagens: COL2, COL10, COL1 (All green). Immunofluorescent images counterstained with DAPI (Blue). Abbreviations are reference for all Figure 4 panels; FH, femur head; AC, articular cartilage; SOC, secondary ossification center; GP, growth plate; P.Sp, primary spongiosa

Remarkably, in contrast to the SOC, COL1 expression was not detected during active mineralization in the FH. In agreement with delayed chondrocyte maturation at the FH of *Tshr*$^{-/-}$ mice, the expression domain of COL2 was expanded, while COL10 was decreased compared with stage matched controls (Figure 4A). Thus, the collagen expression profile is consistent with not only the delayed maturation at the FH but also mineralization occurring in a COL1 negative environment, unlike the SOCs at the distal end.

The progressive remodeling of collagens associated with distinct phases of chondrocyte maturation is principally achieved by enzymatic degradation. The key enzyme to preferentially target COL2 destruction is MMP13 (Inada et al., 2004). Immunostaining revealed that on day 10, MMP13 was largely expressed in a non-overlapping domain with COL2, while on days 17 and 21, MMP13 overlapped both COL2 and COL10 in chondrocytes, but minimally overlapped COL1 in bone, and remained expressed in FH of *Tshr*$^{-/-}$ mice (Figure 4B). MMP9 degrades collagens expressed by more mature chondrocytes (Stickens et al., 2004), and while it was detected in bone tissue of all samples including strong expression at the SOC, it was not expressed in FH chondrocytes (Figure 4B).

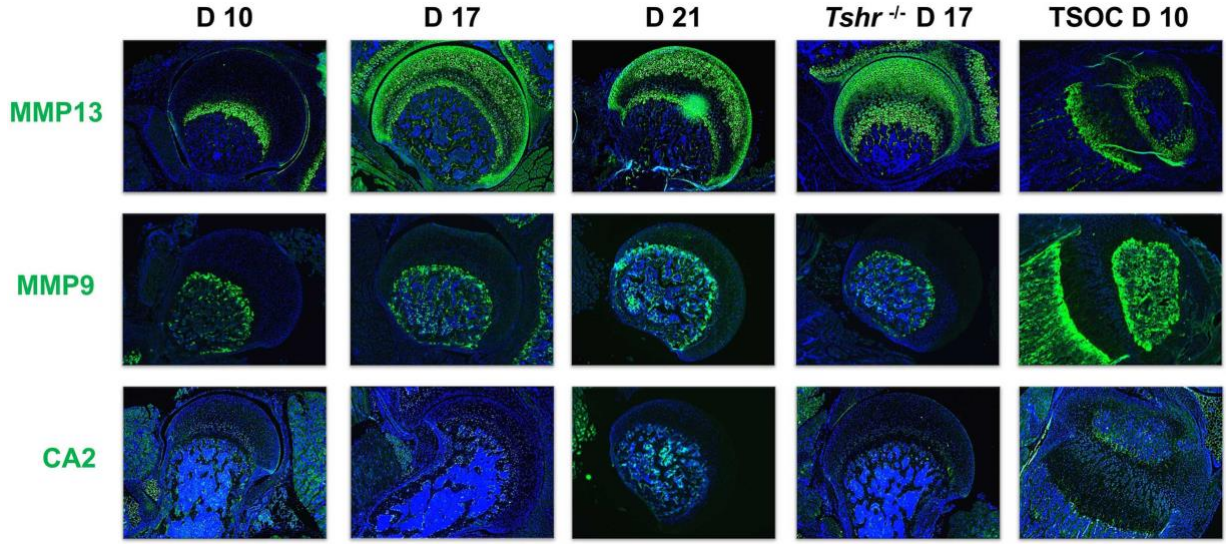

Figure 4B. Immunohistochemical characterization of FH development. Enzymes. Immunofluorescence staining of Enzymes, Matrix Metallopeptidase MMP13, MMP9, CA2 stained in green; counterstained with DAPI (blue).

Osteoblast mineralization is affected by a pH balanced extracellular matrix, the function of which is in part regulated by Carbonic Anhydrase II (CA2) (Adeva-Andany, Fernandez-Fernandez, Sanchez-Bello, Donapetry-Garcia, & Martinez-Rodriguez, 2015). While we found expression of CA2 in osteoblasts at the tibia SOC and in bone beneath the FH, we did not detect its expression in FH chondrocytes (Figure 4B). We also evaluated expression of non-collagenous extracellular matrix proteins involved in mineralization, BSP, OCN, DMP1, and OPN. They were all expressed highly in the SOC and bone below the FH at all time points analyzed, and only OCN was found in D10 FH. On days 17 and 21 OCN expression was lower in FH than in the bone matrix below the FH. While there was some positive signal for BSP in the FH on days 17 and

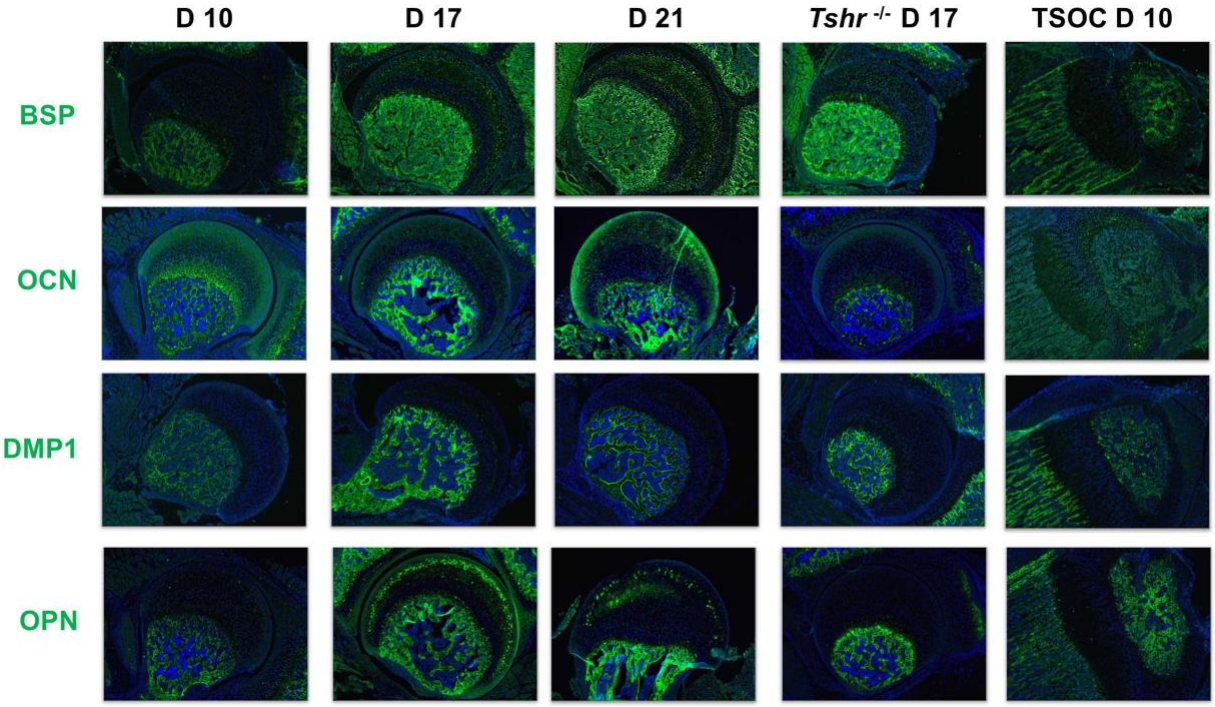

Figure 4C. Immunohistochemical characterization of FH development. Immunofluorescence staining of Non-collagenous extracellular matrix proteins. BSP, OCN, Dentin Matrix Protein 1 (DMP1), and OPN stained in green; samples were counterstained with DAPI (blue).

21, the signal intensity was much less than seen in the bone beneath the FH chondrocytes. DMP1 was not detected in the FH at any of the days evaluated, and OPN was expressed at high level in mineralizing chondrocytes of *Tshr*$^{+/-}$ control FH on day 17 (Figure 4C). None of these mineralization factors were expressed in *Tshr* $^{-/-}$ FH chondrocytes. ALP activity was detected in bone and mineralizing regions of FH in *Tshr*$^{+/-}$ control mice at day 17 and 21 (Figure 4 Supplement1). These results reveal that some of the players involved in mineralization are differentially expressed in the FH versus SOC.

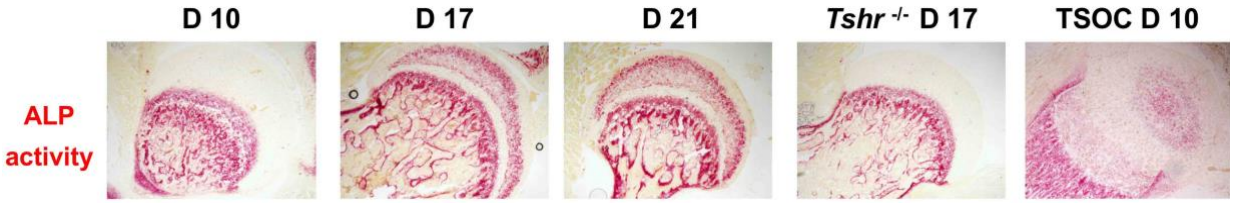

Figure 4 Supplement 1. Alkaline Phosphatase (ALP) activity in FH on Day (D)10, 17, 21, proximal tibia epiphysis on day 10 of *Tshr*$^{+/-}$ controls, and FH of *Tshr*$^{-/-}$ on day 17 FH (red stain).

We next determined if key transcription factors involved in chondrocyte/osteoblast differentiation (SOX9, RUNX2, OSX, DLX3, DLX5, HIF1α) are differentially expressed during mineralization of FH versus distal epiphysis. SOX9 signal was limited to chondrocytes in all regions examined. While SOX9 was not detected in hypertrophic chondrocytes in the tibia growth plate on day 10, it was present throughout the FH at all stages analyzed. RUNX2 was preferentially expressed in osteoblasts of the SOC and maturing chondrocytes at the tibia growth plate, as well as bone in the proximal femur, but not detected in FH chondrocytes until day 17 and thereafter. Both SOX9 and RUNX2

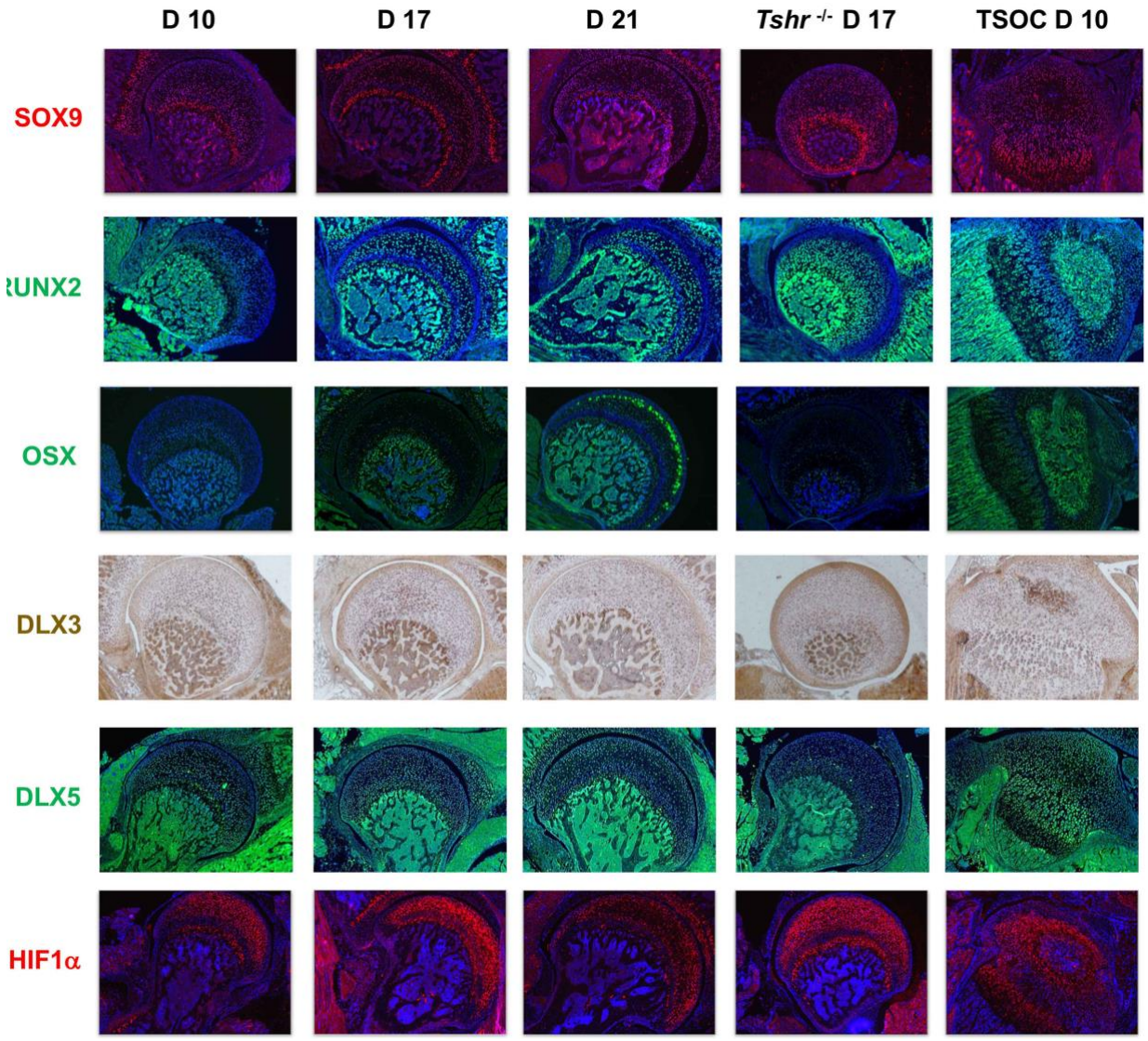

Figure 4D. Immunohistochemical characterization of FH development. Immunofluorescence staining of Transcription Factors. SOX9, HIF1α are stained in red. RUNX2, OSX, and Distal-Less Homeobox 5 (DLX5) are stained in green. Immunofluroescence images counterstained with DAPI (blue). DLX3 stained in brown by colorimetric immunohistochemistry.

were expressed in the FH of *Tshr*$^{-/-}$ mice. Strong OSX expression was detected at the SOC and pre-hypertrophic chondrocytes of the tibia growth plate, as well as bone of proximal tibia, but minimally expressed in FH chondrocytes until day 21, and absent in *Tshr*$^{-/-}$ FH (Figure 4D). Both DLX3 and DLX5 were detected in mineralizing bone both proximally and distally. While DLX3 is expressed in FH chondrocytes prior to and during mineralization, DLX5 expression is weak or absent in the mineralizing region of the FH. HIF1α was expressed in the differentiating chondrocytes of both proximal femur and tibia but to a reduced extent in mineralizing bone. These results reveal that unlike the distal femur where bone is formed by endochondral ossification, OSX likely plays a limited role in the initiation of FH chondrocyte mineralization.

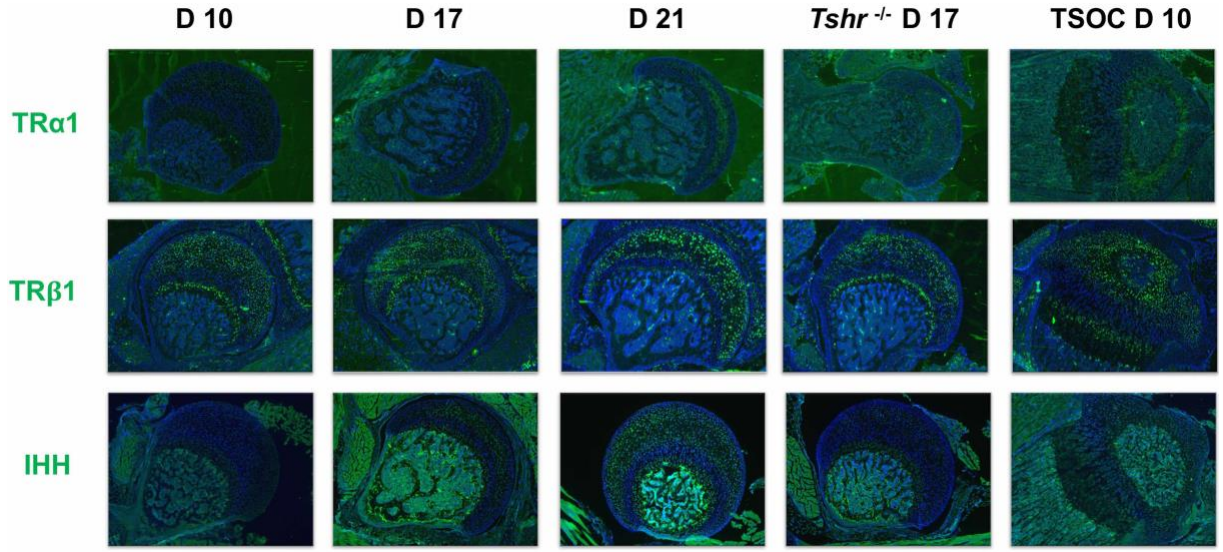

Figure 4E. Immunohistochemical characterization of FH development. Immunofluorescence staining of Thyroid Hormone response factors. Thyroid Hormone Receptor α1 (TRα1), TRβ1, IHH stained green. Counterstained with DAPI (blue)

Since TH is known to be critically involved in regulating chondrocyte maturation, we determined if delayed chondrocyte maturation in the FH can be explained on the basis of differences in TH receptor expression pattern in the FH versus SOC at the proximal tibia. Interestingly, we found that TRα1 was minimally expressed in proximal FH chondrocytes on day 10 but was expressed in day 10 chondrocytes and pre-hypertrophic chondrocytes of the proximal tibia (Figure 4E). A notable gradual increase in expression was then observed on days 17 and 21, and reduced expression was seen in *Tshr*$^{-/-}$. By comparison, TRβ1 was expressed on day 10 FH in subarticular chondrocytes and in an expanded domain at the FH on days 17 and 21, as well as in chondrocytes surrounding

the SOC and in pre-hypertrophic chondrocytes of the growth plate in the proximal tibia (Figure 4E). Consistent with our identification of IHH as a direct target of TH action (Aghajanian et al., 2017; Xing et al., 2016), we found IHH expression in differentiating chondrocytes of both FH and tibia in a pattern that overlapped COL10 expression.

Transcription factor regulation of chondroprogenitor differentiation

Next, we aimed to determine how TH affects chondrocyte differentiation under controlled culture conditions, and how perturbation of master regulator transcription factors (RUNX2, OSX), and their co-regulators (DLX3, DLX5) affect this process in the absence or presence of TH. We therefore knocked down each of these transcription factors in the ATDC5 chondroprogenitor cell line by lentiviral delivery of shRNAs targeting each factor and included a non-specific/random control shRNA. First, we measured the response of ATDC5 cells transduced with control shRNA to a selected panel of genes via RT-qPCR after 3 days of treatment with vehicle or TH in the absence or presence of ascorbic acid (AA), a known inducer of chondrocyte differentiation (Altaf, Hering, Kazmi, Yoo, & Johnstone, 2006) (Figure 5A). Treatment with TH only resulted in significant repression of *Sox9* and *Col2*, as well as induction of *Col10*, and modulators of mineralization, *Bsp*, *Opn*, *Ocn*, *Alp*, and *Dmp1*. By contrast, addition of AA results in significant upregulation of *Runx2* and *Osx,* an effect that was also observed in AA/TH treated cultures. Interestingly, compared with AA alone, treatment with AA/TH repressed *Dlx3* and induced *Dlx5* expression (Figure 5A), as well as *Col10*, *Opn*, *Ocn*, *Alp* and *Dmp1*. These data indicate that TH in general promotes expression of genes involved in chondrocyte maturation and bone mineralization in chondroprogenitors, although TH effects vary in some instances depending on whether AA is present.

The consequence of knockdown of individual transcription factors on various targets is shown in Figure 5B-F. The knockdown of intended targets was validated by data shown in (Figure 5B, Figure 5 Supplement1). In the absence of TH and/or AA treatment, RUNX2, OSX, and DLX3 positively regulate markers of chondrocyte maturation, *Col10*, *Mmp13*, but seem to inhibit expression levels of markers of matrix mineralization, *Bsp*, *Opn*, *Dmp1*, and *Mgp*. Interestingly, expression levels of bone formation markers, *Ocn* and *Alp* are regulated in an antagonistic fashion by DLX3

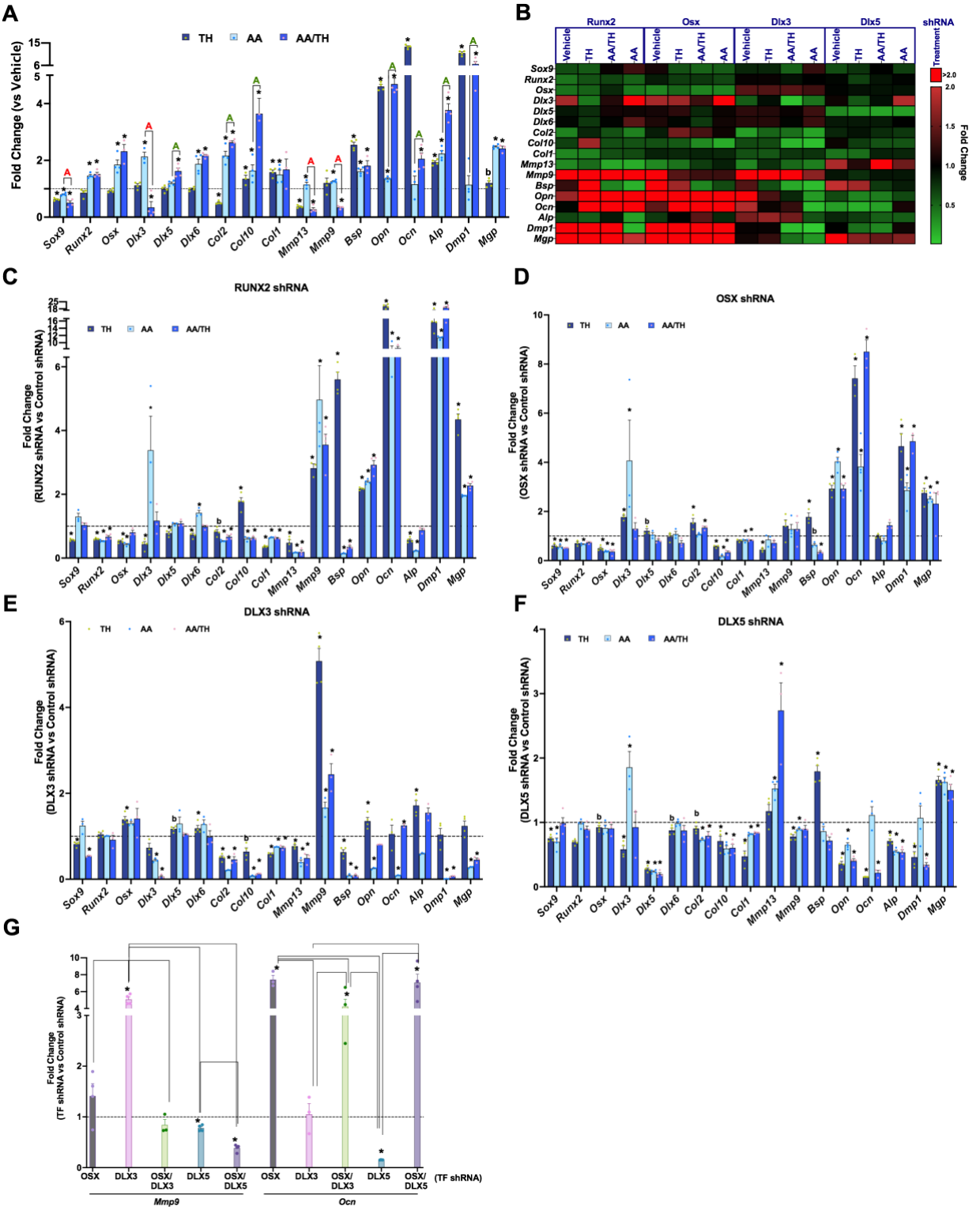

Figure 5. TH and transcription factor regulation of chondroprogenitor genes.
(Panels A-G) RT-qPCR on Day 3 for ATDC5 cell line represented as Fold Change for genes labeled on X-axis. (Panel A) ATDC5 with control shRNA following treatment with TH, AA or AA and TH (AA/TH). (Panel B) Heat map of all 17 genes analyzed in ATDC5 with shRNA for RUNX2, OSX, DLX3, DLX5. Graphed are the response to treatment with Vehicle, TH, AA or AA/TH vs control shRNA. Reduction in

351

expression signifies positive regulation (Green), while increased expression signifies negative regulation (Red). (Panels C-F) Individual transcription factor knockdown vs control shRNA following treatments vs vehicle. (Panel G) Comparison between groups knocked down for a given transcription factor combination on X-axis versus control shRNA in TH treatment at either *Mmp9* or *Ocn*. Statistics analyzed by T-test where * = P<0.05 or less; b = P<0.05-0.10, and in Panel G one way ANOVA where comparison bars indicate P<0.05 or less. (n=4).

(negative) and DLX5 (positive). As expected, knockdown of RUNX2 results in *Osx* downregulation, but not vice versa (Nakashima et al., 2002).

Next, we evaluated whether and how the four transcription factors alter TH's effect on regulation of chondrocyte differentiation by comparing changes elicited by shRNA for each transcription factor with control shRNA while in TH with and without AA. (Figure 5B-5F, Table 1). RUNX2 positively regulates expression of *Sox9*, *Osx*, *Dlx3* and *Dlx5* (Figure 5C), DLX3 negatively regulate expression levels of *Osx* and *Dlx6* (Figure 5E) in control cultures. In the presence of TH, OSX negatively regulates *Dlx3* expression (Figure 5D) while DLX5 positively regulates *Dlx3* expression (Figure 5F). While TH treatment alone represses *Col2* and induces *Col10* and *Col1*, in the presence of AA, TH promotes *Col2* and *Col10* expression, but not *Col1*. In TH treated cultures, *Col10* expression is positively regulated by OSX and DLX5 while RUNX2 is a negative regulator. All four transcription factors positively regulate *Col10* and *Col1* expression in AA/TH treated cultures. DLX3 and OSX exert positive and negative effects respectively on *Col2* expression in the presence of TH. These data suggest that TH promotes maturation of chondrocytes by inhibiting *Sox9* expression and promoting *Col10* expression, which is likely co-regulated by all transcription factors examined.

TH treatment represses *Mmp13* expression regardless of AA involvement (Figure 5A). In TH treated cultures, *Mmp13* is positively regulated by RUNX2, OSX and DLX3, while in AA/TH treated cultures, *Mmp13* is positively regulated by RUNX2 and DLX3 and negatively regulated by DLX5 (Figure 5C, 5E). *Mmp9* was repressed by TH but only in the presence of AA (Figure 5A). *Mmp9* is negatively regulated by RUNX2 and DLX3 in TH+AA treated cultures as well as in control cultures (Figure 5, Figure5 Supplement1). These results indicate that transcription factor regulation of *Mmp13* and *Mmp9* is the same in the presence or absence of TH, but RUNX2 and DLX3 impede TH mediated repression of *Mmp13*, while DLX5 antagonizes the DLX3 effect, and further promotes TH

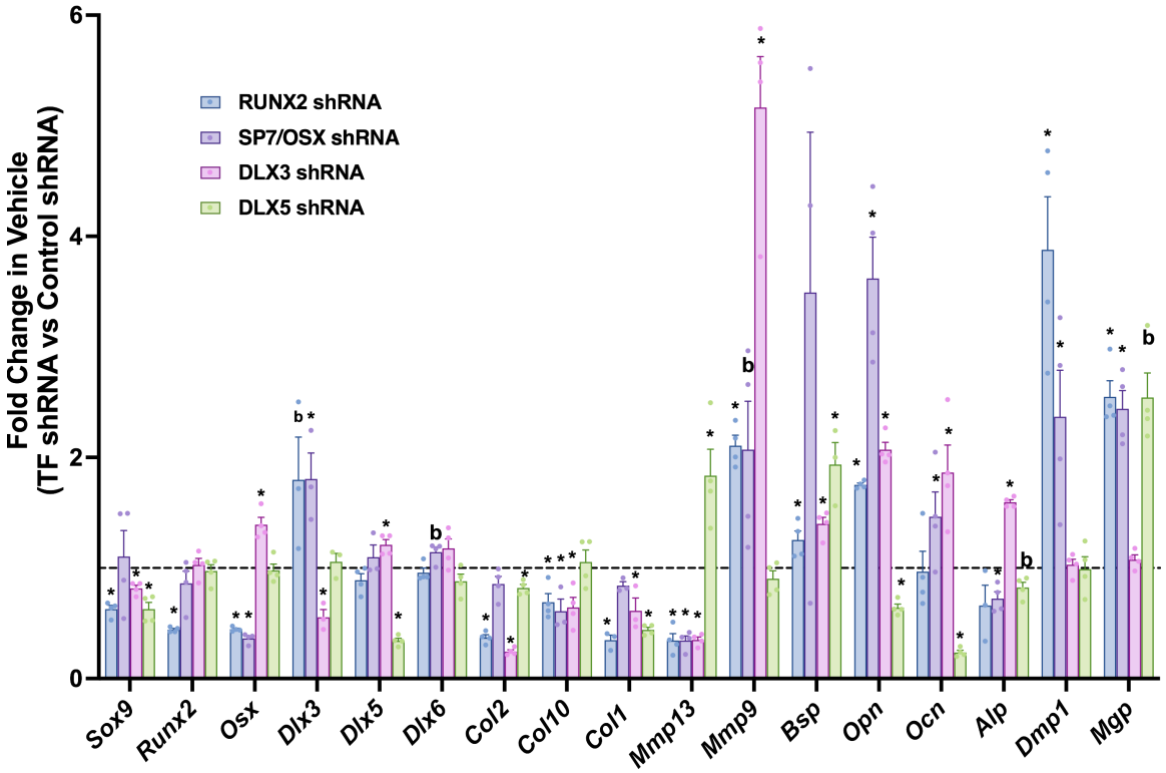

Figure 5 Supplement 1. Effect of individual transcription factor knockdown in vehicle treatment. RT-qPCR on Day 3 for ATDC5 transduced with shRNA for individual transcription factors RUNX2, SP7/OSX, DLX3, or DLX5 comparing fold changes at genes labeled on x-axis vs control shRNA in vehicle treatment condition. Statistics analyzed by T-test where * = P<0.05 or less; b = P<0.05-0.10 (n=4).

	Vehicle treatment		TH treatment		AA+TH treatment		AA treatment	
	Negative	Positive	Negative	Positive	Negative	Positive	Negative	Positive
Sox9		2,3,5		2,3,5,7		7		5,7
Runx2								7
Sp7	3	2	3	2				2
Dlx3		7	7	2,5			2,5,7	
Dlx5	3			2				
Dlx6			2	3			2	
Col2		2,3	7	3	7	2,3,5		2,3,5
Col10		2,3,7	2	5,7		2,3,5,7		2,3,5,7
Col1		2,3,5		2,3,5		2,3,5,7		2,3,5,7
Mmp13	5	2,3,7		2,3,7	5	2,3	5	2,3
Mmp9	2,3		2,3	5	2,3		2,3	5
Bsp	2,3		2,5,7	3		2,3,7		2,3
Opn	2,3,7	5	2,3,7	5	2,7	5	2,7	3,5
Ocn	3	5	2,7	5	2,3,7	5	2,7	3
Alp	3	7	3	2		5		2,5
Dmp1	2,7		2,7	5	2,7	3,5	2,7	3
Mgp	2,7		2,5,7		2,5,7	3	2,5,7	3

Table 1. Comparison of genes regulated by different transcription factors with a p-value <0.05 from Figure 5 panel B after treatment with Vehicle, TH, AA+TH or AA. "Negative" indicates knockdown of a given transcription results in a significant increase of gene in question, while "Positive" indicates the opposite. 2=Runx2; 3= DLX3; 5=DLX5; 7=SP7/OSX shRNAs.

379

mediated repression of *Mmp13*. Also, RUNX2 and DLX3 further promote the negative regulation of *Mmp9* by TH observed in the presence of AA.

TH induced expression of mineralization modulators *Bsp*, *Opn*, *Ocn*, *Alp*, and *Dmp1*, and in this condition, RUNX2 and OSX appear to negatively regulate *Bsp* and *Opn* expression, in collaboration with DLX5 at *Bsp* and DLX3 at *Opn* (Figure 5C-5F). It is interesting that in this condition DLX3 positively regulates *Bsp*, while DLX5 positively regulates *Opn*, which demonstrates their antagonism of key modulators of mineralization in the presence of TH. Similarly, in the presence of TH, *Alp* is positively regulated by RUNX2 and DLX5 and negatively by DLX3. However, in some instances, only one of these co-regulators are active. Such is the case at *Dmp1* which is negatively regulated by RUNX2 and OSX, yet positively regulated by DLX5. DLX5 also promotes TH mediated regulation of the *Ocn* gene, which shows the most robust response to TH treatment in chondrocytes. By contrast, AA effect on *Ocn* gene expression was mediated by DLX3. Overall, these data reveal a complex interplay of transcriptional circuits in ATDC5 chondrocytes treated with TH and/or AA.

Based on the known interaction between OSX and DLX family members and the predicted DLX mediated recruitment of OSX to osteoblast enhancers during osteoblast specification (Hojo, Ohba, He, Lai, & McMahon, 2016), we determined DLX effects in the context of whether OSX is present or absent. Figure 5G shows that the knockdown effect of DLX3 or DLX5 on expression of *Mmp9* and *Ocn* in the presence of TH is differentially affected depending on whether OSX is present or absent. The inhibitory effect of DLX3 on *Mmp9* expression is completely lost in the absence of OSX. However, DLX5 but not DLX3 mediates TH effects on *Ocn* expression in the presence of OSX, and the positive effect of DLX5 on *Ocn* expression is lost when OSX is absent. Overall, these results show that the contribution of gene regulation by co-regulators in response to TH is dependent on master regulators.

Discussion

The salient features of our study are as follows: 1) To our knowledge, this is the first demonstration that TH provides a fundamental input for the timely formation of the proximal femur, and in particular, for chondrocyte maturation and cartilage mineralization at the FH. 2) Overall, this study provides a mechanistic framework to understand the process of cartilage mineralization and how it differs from the endochondral bone formation process. 3) Our understanding of the regulatory molecules and cellular processes involved in ossification of cartilage during normal development may provide important clues to the understanding of components involved in pathological mineralization such as that seen in vascular tissues, and, thereby, provide an opportunity to identify strategies to diagnose and correct soft tissue calcifications.

Our initial characterization of the hip joint in hypothyroid *Tshr*$^{-/-}$ mutant animals led us to investigate the chronological events involved with FH maturation and mineralization. Intriguingly, although TH levels rise systemically, distal knee epiphyseal chondrocytes respond early and undergo endochondral ossification producing a secondary ossification center, while their proximal FH counterparts experience a delay in maturation, that is exacerbated in *Tshr*$^{-/-}$ mice. Our findings that TH injections rescue timely mineralization at the FH of *Tshr*$^{-/-}$ mice provides evidence that TH provides a direct input into this process. Moreover, the detection of TRα1 and downstream genes in FH in euthyroid mice on day 17, when we observe the earliest onset of FH mineralization, suggests TH provides a crucial signal that initiates this process. Indeed, addition of TH to chondrogenic progenitors in culture results in the early induction of several positive and negative modulators of mineralization. Future studies are needed to identify the mechanisms for the delayed expression of TRα1 at the FH compared to distal femur and proximal tibia.

In this study, we have identified interesting differences in the expression levels of extracellular matrix components, enzymes involved in matrix degradation and mineralization, growth factors as well as transcription factors between FH and distal femur during the period when active mineralization occurs in these two regions. While Safranin O and Toluidine Blue staining revealed evidence for the presence of cartilage in the mineralized region of FH at day 21, cartilage staining was absent in the mineralized tissue of distal femur at day 10 (Figure 2). Accordingly, while COL10 was abundantly present

in the mineralizing tissue of FH at day 21, COL10 was absent at the SOC of the distal epiphysis. By contrast, COL1 was abundantly present in the mineralized tissue of the distal epiphysis but was totally absent in the mineralized tissue of the FH. In terms of enzymes, MMP9, CA and TRAP2 were present in the mineralizing region of the distal epiphysis but absent in the FH. MMP9 was identified as a direct target of OSX (Yao et al., 2019). Accordingly, while we found strong OSX expression in the mineralizing tissue at the distal epiphysis, there was little or no signal for OSX in the mineralizing region of the FH. Similarly, DLX5 was strongly expressed in the mineralizing tissue of the distal epiphysis but not in the FH.

To understand the molecular mechanisms for TH regulation of chondrocyte maturation and bone formation, we evaluated the consequence of knockdown of master regulators of endochondral bone formation (RUNX2 and OSX) and their coregulators (DLX3 and DLX5) on TH-induced changes in expression levels of markers of chondrocytes and osteoblasts using ATDC5 chondrocytes. We also evaluated the role of these transcription factors in mediating TH effects in the presence of AA, a known inducer of chondrocyte differentiation (Altaf et al., 2006; Newton et al., 2012). Our data as summarized in Table 1 reveal that while RUNX2 is the main positive regulator of OSX, as expected, we identified DLX3 as a negative regulator of OSX. Interestingly, both COL10 and COL1 expression are positively regulated by all four transcription factors in AA or AA+TH treated cultures. While MMP9 expression was negatively regulated by RUNX2 and DLX3, its expression was positively regulated by DLX5. Furthermore, the negative effect of TH on MGP expression was mediated by RUNX2, DLX5 and OSX while the positive dramatic effects of TH on *Ocn* expression was mainly mediated by DLX5. Additionally, our data involving knockdown of OSX together with DLX3 or DLX5 (Figure 5G) reveal that the positive effect of DLX5 on *Ocn* expression was dependent on whether or not OSX was present, thus revealing that interactions between OSX and DLX factors contribute to transcriptional regulation of bone matrix genes.

Based on the findings presented in this manuscript and the known role of TH in the regulation of endochondral bone formation, we propose the following model to explain the divergent contribution of chondrocytes to endochondral ossification at the distal femur versus direct mineralization of COL10 matrix by chondrocytes at the proximal FH (Figure

6). Despite the prolonged status of an articular chondrocyte-like immature state at the FH, the initial shift towards differentiation is the same at both ends, whereby COL2 and ACAN are degraded by MMP13 and ADAMTs and replaced by COL10 by mature chondrocytes. In this mature state, COL10 mineralization is inhibited distally by TH mediated induction of mineralization inhibitors such as DMP1 and MGP, allowing subsequent degradation of COL10 by MMP9, clearing the way for mineralization of COL1 secreted by osteoblasts. By contrast, at the proximal FH a RUNX2/DLX3 duo represses MMP9 expression, protecting COL10 from degradation. RUNX2 also represses expression of mineralization inhibitors, DMP1 and MGP, thus allowing progression of COL10 mineralization. Lack of COL1 in the FH at the time of mineralization is consistent with the prediction that COL10 represents the major matrix component that is mineralized at this site. However, it remains to be seen if there are other matrix components (e.g. OPN) that also contribute to FH mineralization. During SOC formation at the distal femur, TH induces expression of OPN, BSP and OCN that are primarily mediated by DLX5. Thus, we postulate that while mature chondrocytes transdifferentiate into osteoblasts in

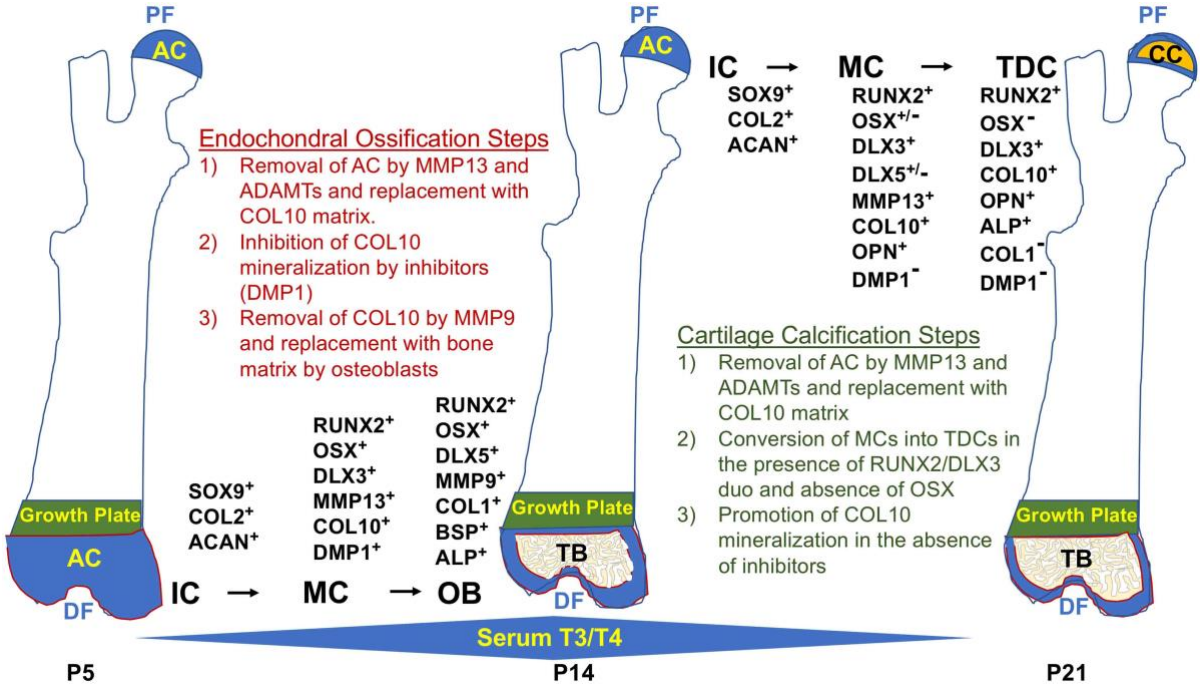

Figure 6. Spatiotemporal model of proximal-distal femoral chondrocyte fate acquisition. Please see text in the discussion for explanation.

Abbreviations: PF, Proximal Femur; AC, Articular Cartilage; CC, Calcified Cartilage; DF, Distal Femur; IC, Immature Chondrocyte; MC, Mature Chondrocyte; TDC, Terminally Differentiated Chondrocyte; OB, Osteoblast; TB, Trabecular Bone; P5-21, Postnatal Day; T3/T4, Thyroid Hormone.

the presence of an OSX and DLX5 duo, which produces bone matrix that promotes endochondral bone formation at the secondary ossification center of the distal femur, RUNX2 in the absence of OSX may interact with DLX3 to promote terminal differentiation of mature chondrocytes and subsequent cartilage mineralization at the FH.

Both master regulators of ossification, RUNX2 and OSX are involved in chondrocyte maturation in different areas that produce bone such as primary ossification centers, secondary ossification and growth plate. Although RUNX2 is upstream of OSX and both may be involved in regulation of genes that promote maturation (Artigas, Urena, Rodriguez-Carballo, Rosa, & Ventura, 2014), at the FH we find that OSX is not notably expressed. Chondrocyte specific knockout of OSX has been reported to result in expanded hypertrophic chondrocyte mineralization (Jing et al., 2014; Zhou et al., 2010), demonstrating that OSX is not required for chondrocyte mineralization, and its timely absence may even affect the fate of RUNX2+ hypertrophic chondrocytes. Incidentally, forced expression of RUNX2 is sufficient to increase the rate of chondrocyte maturation and induce ectopic chondrocyte mineralization in vivo (Takeda, Bonnamy, Owen, Ducy, & Karsenty, 2001). Also, OSX has been shown to be a positive regulator of COL1 and its interaction with DLX5 was shown to be critical for osteoblast specification (Hojo et al., 2016; Ortuno, Susperregui, Artigas, Rosa, & Ventura, 2013). Our findings support the model that an OSX/DLX5 duo contribute to transdifferentiation of chondrocytes to osteoblasts at the distal femur during endochondral bone formation, and the limited activity of OSX at the proximal femur may partly explain the difference in fates there.

We sought to understand why chondrocyte maturation at the proximal FH is delayed compared with the distal femur. One possibility is a difference in endothelial vasculature, but distal femur chondrocytes mature in response to TH prior to expression of VEGF (Aghajanian et al., 2017), limiting this option. We searched whether VEGF is expressed in the FH but did not detect it (data not shown), consistent with results reported by Cole et al. (2013). Therefore, the presence of HIF1α+/VEGF- chondrocytes support the notion that HIF1α does not regulate VEGF expression in this context, but is likely promoting collagen hydroxylation or contributing to chondrocyte metabolism (Bentovim, Amarilio, & Zelzer, 2012). Another possibility is that TH might regulate growth factor expression differentially in chondrocytes at the two ends of the femur, as shown by our

data on *Tgfα* (Figure 3A). It is equally possible that TH mediated activation or repression of signals from adjacent structures can affect the timing of maturation and mineralization at the proximal FH. Alternatively, TH activity might be subdued early at the FH. Indeed, we found that the thyroid hormone receptor, TRα1, was highly expressed distally on day 10, but minimally at the FH in the same mice at postnatal day 10. In this regard, a complementary pattern was noted for the expression of IHH, a direct target of TH at both ends, supporting the likelihood that delayed chondrocyte development at the FH is caused by reduced TH activity. Addressing this question further will be worthwhile for future investigations.

The potential clinical relevance of our findings are as follows: it is known that physiological mineralization is necessary for the formation of skeletal tissues and is restricted to specific sites in skeletal tissues including cartilage, bone and teeth. Mineralization can also occur in an uncontrolled or pathological manner in many soft tissues including cardiovascular, kidney and articular cartilage leading to morbidity and mortality. Recent studies focused on the underlying mechanisms for vascular calcification have shown that components regulating physiological mineralization are also present in areas of pathological mineralization (Bourne, Wheeler-Jones, & Orriss, 2021; Tesfamariam, 2019), suggesting that mechanisms for pathological mineralization may be a recapitulation of what happens during normal development. Therefore, studies focused on the understanding of regulatory molecules and cellular processes involved in ossification of cartilage and bone tissues during normal development may provide important clues toward the understanding of components involved in pathological mineralization. Our further confirmation of the role of molecular signals and mechanisms that contribute to TH effects on cartilage versus bone mineralization at FH and distal femur, respectively, could lead to the development of novel strategies for prevention and treatment of osteoarthritis and other soft tissue calcification disorders.

Materials and Methods

Mouse model

We obtained the *Tshr*^{hyt} mouse strain from Jackson Laboratories (Bar Harbor, ME). Animals were inbred and tail snip extracted DNA was genotyped for *Tshr* mutation by RT-qPCR. Mice were housed in standard housing conditions at the VA Loma Linda Healthcare System Veterinary Medical Unit (Loma Linda, CA). All procedures were approved by the Institutional Animal Care and Use Committees of the VA Loma Linda Healthcare System. At time of sacrifice, mice were anesthetized in isoflurane, then exposed to CO_2 prior to cervical dislocation, and bones dissected for further processing. For TH replacement experiments, genotyped mice were injected intraperitoneally with 1μg T3 and 10μg thyroxine (T4) [Sigma-Aldrich], or an equal volume of vehicle (5mM NaOH) for 10 days (on days 5-14). Bones of mice studied on day 10 were injected on days 5-9 and sacrificed on day 10. *Tshr* mice do not show gender differences until 5 or 6 weeks. Therefore, mice were pooled regardless of gender in all analysis.

X-ray

Femur X-rays of anesthetized hypothyroid *Tshr* $^{-/-}$ and euthyroid *Tshr* $^{+/-}$ mice were obtained from Faxitron Radiography system (Hologic, USA) at postnatal day 21 using 20kV X-ray energy for 10 seconds.

Micro CT

Proximal femurs were evaluated by μCT (viva CT40; Scanco Medical, Switzerland) as described previously (Xing et al., 2014). Proximal femurs were isolated from postnatal day 21, fixed in 10% formalin overnight (ON), then washed and imaged in phosphate buffered saline (pH 7.4). Bones were scanned by X-ray at 55 kVp volts at a resolution of 10.5 μM/slice. Images were reconstructed using the 2-D and 3-D image software provided by Scanco Viva-CT 40 instrument (Scanco, USA, Wayne, PA).

nanoCT

Proximal and distal femurs of *Tshr*$^{+/-}$ mice were scanned at postnatal day 10, 14, 17 and 21 using a nano-CT at a voxel dimension of 0.3 µm (VersaXRM-500; Xradia, Pleasanton, CA, USA). Images were captured using software provided by Xradia.

Histology

Mouse femurs were fixed in 10% formalin overnight, washed, decalcified in 10% EDTA (pH 7.4) at 4 C for 7 days with shaking and embedded in paraffin for sectioning. Longitudinal sections of the proximal and distal femur were stained with various stains using standard procedures.

Immunohistology

Longitudinal 5µM sections at regions of interest shown in figures were obtained by immunofluorescence following standard protocols. Both paraffin and cryosections were processed. Dissected bones were fixed for 3 days in either 10% formalin (paraffin) or 4% paraformaldehyde (cryosections) at 4°C, followed by one week of de-calcification in 20% EDTA in PBS buffer (pH 7.5). Cryosectioned samples were embedded and sectioned in OCT (FisherScientific, 23-730-571). Paraffin sections were deparaffinized in Histochoice clearing reagent (Amresco, H103-4L), gradually re-hydrated in ethanol through PBS, then permeabilized in 0.5% Triton X-100 (SIGMA, T-9284) for 15 minutes at RT, rinsed in PBS, followed by an antibody specific antigen retrieval approach (see Methods Table 1). Cryosections were processed identically except they were thawed to RT then started at the permeabilization step. Following antigen retrieval, tissue sections were blocked in 2.5% serum and incubated in primary antibodies ON at RT. Commercial species-specific secondary antibodies were used (VECTOR labs, DI-1788 or DI-3088), and sections were counterstained with DAPI (Invitrogen, D1306). Colorimetric immunohistochemistry followed same steps as for immunofluorescence except 1) endogenous peroxidase was quenched with 3% H_2O_2 prior to permeabilization 2) biotinylated goat anti-rabbit HRP secondary antibody was added at 1:200 (Vector BA-1000), followed by a 1:200 dilution of streptavidin-HRP (Vector: SA-5004), and detected by enzyme reaction with Betazoid DAB chromogen (BIOCARE BDB2004H). The Vector lab's mouse on mouse (MOM) kit

(BMK-2202) was used with mouse primary antibodies according to manufacturer instructions. Other VECTOR reagents used with MOM kit: Avidin/Biotin block, #SP-2001; Fluorescein Avidin #DCS A-2011.

Microscopy

Immunofluorescence images were obtained on a 5X dry objective on a Leica Digital Microscope DMI6000B with Leica Application Suite X software. Histological and colorimetric immunohistochemical images were obtained on an Olympus microscope with an Olympus DP72 camera with DP2-BSW software. All immunohistological results were processed together with consecutive sections that either received no primary antibody or species-specific IgG antibody. These were imaged at identical parameters as sections probed with antibodies.

ALP Histochemistry

Alp activity assay was performed on cryo-sectioned samples as described (Miao & Scutt, 2002). Sections were warmed to room temperature, OCT compound washed out, then incubated in ALP buffer (6.055g Tris; 5.84g NaCl; 0.147g CaCl2•2$H_2$0; 0.372g KCl; 0.203g $MgCl_2$•6$H_2$0 in 1L H20 pH 8.6) containing 1% magnesium chloride at 4°C O/N. Next day, samples were directly transferred to ALP buffer + Substrate (0.2 mg/mL naphthol AS-MX phosphate [Sigma-Aldrich, N6125-1G] and 0.4 mg/mL Fast Red violet LB [Sigma-Aldrich, F3381-1G]). Reaction was monitored, sections were rinsed with PBS, and imaged immediately. All samples received identical reaction time.

Cell culture

ATDC5 chondrocyte cell line was purchased from the American Type Culture Collection (Manassas, VA). Cells were maintained in DMEM-F12 medium containing 5% FBS, penicillin (100 U/mL), and streptomycin (100μg/mL) at 5% CO_2 in normoxic conditions at 37°C. Cells were incubated in the presence of serum-free DMEM-F12 medium containing 0.1% bovine serum albumin (BSA) and antibiotics for 24 h prior to treatment with 10ng/mL T3 (Sigma-Aldrich), 50 μg/mL Ascorbic Acid and/or 10mM β-Glycerol phosphate (BG). Vehicle control indicate cells treated with BG only. shRNA knockdown was achieved by

transduction of Mission Lentiviral particles (Millipore, Sigma): Control shRNA-Cat#SHC002V; RUNX2 NM_009820, Cat#TRCN0000095590; DLX3 NM_010055, Cat#TRCN0000430532; DLX5 NM_010056.2 Cat#TRCN0000428940; Sp7 NM_130458 Cat#TRCN0000423959

Real Time quantitative PCR (RTqPCR)

RNA was extracted from epiphyseal chondrocytes or ATDC5 cells in TRI reagent (Molecular Research Center INC, TR118) according to manufacturer instructions, and purified on silica columns with E.Z.N.A. Total RNA Kit I (Omega BIO-TEK, R6834-02). Total RNA was reverse transcribed to cDNA with oligo(dT)$_{12\text{-}18}$ and Superscript IV Reverse transcriptase (Invitrogen, 18091050). A final concentration of 0.133ng/μL was used per real time PCR reaction with InVitrogen SYBR green (ThermoFisher, 4309155) and processed on a ViiA 7 RT-PCR system. All reactions were standardized with Peptidyl prolyl isomerase A (PPIA) primers. Primer sequences used for RT-qPCR are listed in Methods Table 2. Fold changes were calculated by the Delta Ct method, and statistics analyzed by T-test (processed on Microsoft Excel 365) or one-way ANOVA (processed on Graphpad Prism9). Error bars in all graphs indicate +/- Standard Error of Mean (SEM).

Author contributions. SM conceived and directed the project. SM, PA and GG designed the experiments and interpreted the data. Experiments were performed by PA, GG, SP and DL. Data analyses were performed by GG, SP and DL. SM and GG wrote the manuscript, and all authors reviewed the manuscript. SM and GG accept responsibility for the integrity of data analysis.

Acknowledgements. This work was supported by National Institutes of Health Grant R01 AR048139 (SM), R21 AG062866 (SM) and Veterans Administration BLR&D Grant BX005263 (SM). SM is a recipient of Senior Research Career Scientist Award from Veterans Administration. The authors thank Veterans Administration for providing facilities to perform the work. Expert technical assistance by Catrina Godwin, Fern Baedyananda, Jasmine Lau, Subhashri Das, Heather Watt and Nancy Lowen are greatly acknowledged.

References

Adeva-Andany, M. M., Fernandez-Fernandez, C., Sanchez-Bello, R., Donapetry-Garcia, C., & Martinez-Rodriguez, J. (2015). The role of carbonic anhydrase in the pathogenesis of vascular calcification in humans. *Atherosclerosis, 241*(1), 183-191. doi:10.1016/j.atherosclerosis.2015.05.012

Aghajanian, P., Xing, W., Cheng, S., & Mohan, S. (2017). Epiphyseal bone formation occurs via thyroid hormone regulation of chondrocyte to osteoblast transdifferentiation. *Sci Rep, 7*(1), 10432. doi:10.1038/s41598-017-11050-1

Altaf, F. M., Hering, T. M., Kazmi, N. H., Yoo, J. U., & Johnstone, B. (2006). Ascorbate-enhanced chondrogenesis of ATDC5 cells. *Eur Cell Mater, 12*, 64-69; discussion 69-70. doi:10.22203/ecm.v012a08

Artigas, N., Urena, C., Rodriguez-Carballo, E., Rosa, J. L., & Ventura, F. (2014). Mitogen-activated protein kinase (MAPK)-regulated interactions between Osterix and Runx2 are critical for the transcriptional osteogenic program. *J Biol Chem, 289*(39), 27105-27117. doi:10.1074/jbc.M114.576793

Bassett, J. H., Williams, A. J., Murphy, E., Boyde, A., Howell, P. G., Swinhoe, R., . . . Williams, G. R. (2008). A lack of thyroid hormones rather than excess thyrotropin causes abnormal skeletal development in hypothyroidism. *Mol Endocrinol, 22*(2), 501-512. doi:10.1210/me.2007-0221

Bentovim, L., Amarilio, R., & Zelzer, E. (2012). HIF1alpha is a central regulator of collagen hydroxylation and secretion under hypoxia during bone development. *Development, 139*(23), 4473-4483. doi:10.1242/dev.083881

Bourne, L. E., Wheeler-Jones, C. P., & Orriss, I. R. (2021). Regulation of mineralisation in bone and vascular tissue: a comparative review. *J Endocrinol, 248*(2), R51-R65. doi:10.1530/JOE-20-0428

Cheng, S., Aghajanian, P., Pourteymoor, S., Alarcon, C., & Mohan, S. (2016). Prolyl Hydroxylase Domain-Containing Protein 2 (Phd2) Regulates Chondrocyte Differentiation and Secondary Ossification in Mice. *Sci Rep, 6*, 35748. doi:10.1038/srep35748

704 Cheng, S., Pourteymoor, S., Alarcon, C., & Mohan, S. (2017). Conditional Deletion of the
705 Phd2 Gene in Articular Chondrocytes Accelerates Differentiation and Reduces
706 Articular Cartilage Thickness. *Sci Rep, 7*, 45408. doi:10.1038/srep45408
707 Cole, H. A., Yuasa, M., Hawley, G., Cates, J. M., Nyman, J. S., & Schoenecker, J. G.
708 (2013). Differential development of the distal and proximal femoral epiphysis and
709 physis in mice. *Bone, 52*(1), 337-346. doi:10.1016/j.bone.2012.10.011
710 Gogakos, A. I., Duncan Bassett, J. H., & Williams, G. R. (2010). Thyroid and bone. *Arch*
711 *Biochem Biophys, 503*(1), 129-136. doi:10.1016/j.abb.2010.06.021
712 Hojo, H., Ohba, S., He, X., Lai, L. P., & McMahon, A. P. (2016). Sp7/Osterix Is Restricted
713 to Bone-Forming Vertebrates where It Acts as a Dlx Co-factor in Osteoblast
714 Specification. *Dev Cell, 37*(3), 238-253. doi:10.1016/j.devcel.2016.04.002
715 Inada, M., Wang, Y., Byrne, M. H., Rahman, M. U., Miyaura, C., López-Otín, C., & Krane,
716 S. M. (2004). Critical roles for collagenase-3 (Mmp13) in development of growth
717 plate cartilage and in endochondral ossification. *Proc Natl Acad Sci U S A, 101*(49),
718 17192-17197. doi:10.1073/pnas.0407788101
719 Jing, J., Hinton, R. J., Jing, Y., Liu, Y., Zhou, X., & Feng, J. Q. (2014). Osterix couples
720 chondrogenesis and osteogenesis in post-natal condylar growth. *J Dent Res,*
721 *93*(10), 1014-1021. doi:10.1177/0022034514549379
722 Kim, H. Y., & Mohan, S. (2013). Role and Mechanisms of Actions of Thyroid Hormone on
723 the Skeletal Development. *Bone Res, 1*(2), 146-161. doi:10.4248/BR201302004
724 Li, J., & Dong, S. (2016). The Signaling Pathways Involved in Chondrocyte Differentiation
725 and Hypertrophic Differentiation. *Stem Cells Int, 2016*, 2470351.
726 doi:10.1155/2016/2470351
727 Mackie, E. J., Tatarczuch, L., & Mirams, M. (2011). The skeleton: a multi-functional
728 complex organ: the growth plate chondrocyte and endochondral ossification. *J*
729 *Endocrinol, 211*(2), 109-121. doi:10.1530/JOE-11-0048
730 Miao, D., & Scutt, A. (2002). Histochemical localization of alkaline phosphatase activity in
731 decalcified bone and cartilage. *J Histochem Cytochem, 50*(3), 333-340.
732 doi:10.1177/002215540205000305
733 Mohan, S., Richman, C., Guo, R., Amaar, Y., Donahue, L. R., Wergedal, J., & Baylink, D.
734 J. (2003). Insulin-like growth factor regulates peak bone mineral density in mice by

both growth hormone-dependent and -independent mechanisms. *Endocrinology, 144*(3), 929-936. doi:10.1210/en.2002-220948

Nakashima, K., Zhou, X., Kunkel, G., Zhang, Z., Deng, J. M., Behringer, R. R., & de Crombrugghe, B. (2002). The novel zinc finger-containing transcription factor osterix is required for osteoblast differentiation and bone formation. *Cell, 108*(1), 17-29. doi:10.1016/s0092-8674(01)00622-5

Newton, P. T., Staines, K. A., Spevak, L., Boskey, A. L., Teixeira, C. C., Macrae, V. E., . . . Farquharson, C. (2012). Chondrogenic ATDC5 cells: an optimised model for rapid and physiological matrix mineralisation. *Int J Mol Med, 30*(5), 1187-1193. doi:10.3892/ijmm.2012.1114

Ortuno, M. J., Susperregui, A. R., Artigas, N., Rosa, J. L., & Ventura, F. (2013). Osterix induces Col1a1 gene expression through binding to Sp1 sites in the bone enhancer and proximal promoter regions. *Bone, 52*(2), 548-556. doi:10.1016/j.bone.2012.11.007

Patton, J. T., & Kaufman, M. H. (1995). The timing of ossification of the limb bones, and growth rates of various long bones of the fore and hind limbs of the prenatal and early postnatal laboratory mouse. *J Anat, 186 (Pt 1)*(Pt 1), 175-185.

Schipani, E., Ryan, H. E., Didrickson, S., Kobayashi, T., Knight, M., & Johnson, R. S. (2001). Hypoxia in cartilage: HIF-1alpha is essential for chondrocyte growth arrest and survival. *Genes Dev, 15*(21), 2865-2876. doi:10.1101/gad.934301

Stickens, D., Behonick, D. J., Ortega, N., Heyer, B., Hartenstein, B., Yu, Y., . . . Werb, Z. (2004). Altered endochondral bone development in matrix metalloproteinase 13-deficient mice. *Development, 131*(23), 5883-5895. doi:10.1242/dev.01461

Takarada, T., Nakazato, R., Tsuchikane, A., Fujikawa, K., Iezaki, T., Yoneda, Y., & Hinoi, E. (2016). Genetic analysis of Runx2 function during intramembranous ossification. *Development, 143*(2), 211-218. doi:10.1242/dev.128793

Takeda, S., Bonnamy, J. P., Owen, M. J., Ducy, P., & Karsenty, G. (2001). Continuous expression of Cbfa1 in nonhypertrophic chondrocytes uncovers its ability to induce hypertrophic chondrocyte differentiation and partially rescues Cbfa1-deficient mice. *Genes Dev, 15*(4), 467-481. doi:10.1101/gad.845101

765 Tesfamariam, B. (2019). Involvement of Vitamin K-Dependent Proteins in Vascular
766 Calcification. *J Cardiovasc Pharmacol Ther, 24*(4), 323-333.
767 doi:10.1177/1074248419838501
768 Wang, L., Shao, Y. Y., & Ballock, R. T. (2010). Thyroid hormone-mediated growth and
769 differentiation of growth plate chondrocytes involves IGF-1 modulation of beta-
770 catenin signaling. *J Bone Miner Res, 25*(5), 1138-1146. doi:10.1002/jbmr.5
771 Wang, Y., Nishida, S., Sakata, T., Elalieh, H. Z., Chang, W., Halloran, B. P., . . . Bikle, D.
772 D. (2006). Insulin-like growth factor-I is essential for embryonic bone development.
773 *Endocrinology, 147*(10), 4753-4761. doi:10.1210/en.2006-0196
774 Xing, W., Aghajanian, P., Goodluck, H., Kesavan, C., Cheng, S., Pourteymoor, S., . . .
775 Mohan, S. (2016). Thyroid hormone receptor-beta1 signaling is critically involved
776 in regulating secondary ossification via promoting transcription of the Ihh gene in
777 the epiphysis. *Am J Physiol Endocrinol Metab, 310*(10), E846-854.
778 doi:10.1152/ajpendo.00541.2015
779 Xing, W., Cheng, S., Wergedal, J., & Mohan, S. (2014). Epiphyseal chondrocyte
780 secondary ossification centers require thyroid hormone activation of Indian
781 hedgehog and osterix signaling. *J Bone Miner Res, 29*(10), 2262-2275.
782 doi:10.1002/jbmr.2256
783 Yao, B., Wang, J., Qu, S., Liu, Y., Jin, Y., Lu, J., . . . Ma, C. (2019). Upregulated osterix
784 promotes invasion and bone metastasis and predicts for a poor prognosis in breast
785 cancer. *Cell Death Dis, 10*(1), 28. doi:10.1038/s41419-018-1269-3
786 Yellowley, C. E., & Genetos, D. C. (2019). Hypoxia Signaling in the Skeleton: Implications
787 for Bone Health. *Curr Osteoporos Rep, 17*(1), 26-35. doi:10.1007/s11914-019-
788 00500-6
789 Zhou, X., Zhang, Z., Feng, J. Q., Dusevich, V. M., Sinha, K., Zhang, H., . . . de
790 Crombrugghe, B. (2010). Multiple functions of Osterix are required for bone growth
791 and homeostasis in postnatal mice. *Proc Natl Acad Sci U S A, 107*(29), 12919-
792 12924. doi:10.1073/pnas.0912855107
793
794
795

796 **Methods Table 1. Antibodies used in this study**

	Vendor	Catalog#	dilution	Antigen Retreival
COL2	DSHB	CIIC1	1:10	HD
COL10	Abcam	ab58632	1:100	HD
COL1	Novus Biologicals	NB600-408	1:100	HD
MMP13	Novus Biologicals	NBP1-45723	1:200	HD
MMP9	Abcam	ab388898	1:100	L
CA2	GeneTex	GTX53908	1:100	HD
BSP	Dr. Renny Franceschi	University of Michigan	1:100	HD
OCN	Abcam	ab93876	1:250	HD
DMP1	Novus Biologicals	NBP1-89484	1:100	HD
OPN	Kerafast	ENH094-FP	1:300	HD
SOX9	Sigma-Aldrich	AB5535	1:100	S
RUNX2	Abcam	ab192256	1:250	S
OSX	Santa Cruz Biotechnology	sc-22536-r	1:50	HD
DLX3	Abcam	ab64953	1:50	HD
DLX5	Abcam	ab109737	1:100	S
HIF1α	Novus Biologicals	NB-100134	1:50	S
TRα1	Santa Cruz Biotechnology	sc-10819	1:50	S
TRβ1	Santa Cruz Biotechnology	sc-10822	1:200	HD
IHH	Abcam	ab39634	1:50	S

Antigen Retrieval with

HD = 2mg/mL Hyaluronidase (Sigma Aldrich) in PBS at 37°C for 45 minutes

S = 10mM Sodium Citrate w/2mM EDTA and 0.05% Tween-20 (pH 6.0) at 95°C for 6 minutes

L = 10mM Sodium Citrate w/2mM EDTA and 0.05% Tween-20 (pH 6.0) at 60°C for 72 hours

797

798

799

800

801

802

803

804

805

806

807 **Methods Table 2. Real Time quantitative PCR Primers used in this study**

Gene		**Primer Sequences**
Adamts4	F	CAGTGCCCGATTCATCACTGA
	R	GAGTCAGGACCGAAGGTCAG
Adamts5	F	CGAAGAGCACTACGATGCAGC
	R	GCATGGAGGCCATCATCTTCAAT
Acan	F	GACCAGGAAGGGAGGAGTAG
	F	CAGCCGAGAAATGACACC
Alp	R	ATGGTAACGGGCCTGGCTACA
	F	AGTTCTGCTCATGGACGCCGT
βcat	F	AGAAGTATGAGGAGCCTCTG
	R	CAGCCTCTGCATCATCATGT
Bmp2	F	GATCTGTACCGCAGGCACTC
	R	GAAACTCGTCACTGGGGACA
Bsp	F	AACGGGTTTCAGCAGACAACC
	R	TAAGCTCGGTAAGTGTCGCCA
Col1	F	GCCTCCCAGAACATCACCTA
	R	AGTTCCGGTGTGACTCGTG
Col2	F	TGGCTTCCACTTCAGCTATG
	R	AGGTAGGCGATGCTGTTCTT
Col10	F	ACGGCACGCCTACGATGT
	R	CCATGATTGCACTCCCTG
Dlx3	F	CACCTACCACCACCAGTTCAA
	R	GCTCCTCTTTCACCGACACTG
Dlx5	F	AGAAGAGTCCCAAGCATCCGA
	R	GCCATAAGAAGCAGAGGTAGG
Dlx6	F	TTCCCGAGAGAGCCGAACT
	R	GTGGGTTACTACCCTGCTTCA
Dmp1	F	TCCAGCTCAGAAAGCCAGTCC
	R	AGAACGGCTGTCCTGCTCAGA
Hif1α	F	TGACGGCGACATGGTTTACA
	R	ACTAAACACACAGCGGAGCT
Hif2α	F	TCATTGCTGTGGTGACCCAA
	R	AGAGCAAAGACGTGTCCACC
Ihh	F	CCCCAACTACAATCCCGACATC
	R	CGCCAGCAGTCCATACTTATTTCG
Mgp	F	CCTGTGCTACGAATCTCACGAA
	R	TCGCAGGCCTCTCTGTTGAT
Mmp9	F	CCATGCACTGGGCTTAGATCAT
	R	CAGATACTGGATGCCGTCTATGTC
Mmp13	R	CATCCATCCCGTGACCTTAT
	F	TCATAACCATTCAGAGCCCA
Ocn	F	CTCTCTCTGCTCACTCTGCT

	R	TTTGTAGGCGGTCTTCAAGC
Opg	F	TGACCTCTGTGAAAGCAGCGTG
	R	GCCCTTCAAGGTGTCTTGGTCA
Opn	F	TACAGTCGATGTCCCCAACG
	R	TGATCAGAGGGCATGCTCAG
Osx	F	TCCTCTCTGCTTGAGGAAGAAG
	R	GAGTCCATTGGTGCTTGAGAAG
Rankl	F	GACTCCTGCAGGAGGATGAA
	R	GTCCTCTTGGTACCACGATC
Runx2	F	AAAGCCAGAGTGGACCCTTCCA
	R	ATAGCGTGCTGCCATTCGAGGT
Shh	F	GCCTACAAGCAGTTTATTCCCA
	R	GTGAGTTCCTTAAATCGTTCGG
Sox9	F	CGGAGGAAGTCGGTGAAGA
	R	GTCGGTTTTGGGAGTGGTG
Tgfα	F	AGCGCTGGGTATCCTGTTAG
	R	CAAAAACCGGCAGGTTCCAT
Trap2	F	CTGCAGGTTGTGGTCATGTCC
	R	CACTCAGCTGTCCTGGCTCAA
Vegf	F	ATATCAGGCTTTCTGGATTAAGGAC
	R	CAGACGAAAGAAAGACAGAACAAAG

808